Struct Chem
DOI 10.1007/s11224-009-9579-9

ORIGINAL RESEARCH

Simvastatin: structure solution of two new low-temperature phases from synchrotron powder diffraction and ss-NMR

Michal Hušák · Bohumil Kratochvíl · Alexandr Jegorov · Jiří Brus · Jaroslav Maixner · Jan Rohlíček

Received: 22 September 2009 / Accepted: 22 December 2009

Abstract Simvastatin is a substance used for the treatment of hypercholesterolemia. In addition to the already known room temperature structure of simvastatin (Čejka et al. in Acta Cryst C59:o428, 2003) two new low-temperature polymorphs were found by X-ray powder diffraction with the phase transition at 261 and 223 K (later confirmed by DSC to be 272 and 232 K). The main differences among three polymorphs consist in the side-chains conformation only and the phase changes are fully reversible. The structures of the polymorphs were studied by the powder diffraction based on synchrotron radiation as well as by solid-state NMR spectroscopy.

Keywords Crystal structure · Simvastatin · Powder diffraction · Solid-state NMR

Introduction

A primary risk factor for the coronary artery disease is known to be hypercholesterolemia. Since in humans 50% or more of the total body cholesterol is derived from de novo synthesis, the enzyme 3-hydroxy-3-methylglutaryl-coenzyme A (HMG-CoA) reductase (EC 1.1.1.34) catalyzing a rate-limiting step in the cholesterol biosynthesis is, therefore, a prime target for pharmacological intervention. The aim of this study is to describe the new low-temperature phases of semisynthetic inhibitor of HMG-CoA reductase simvastatin (Scheme 1).

As is often observed pharmaceutical solids can exhibit extensive polymorphism. Technologically, this is crucial since structural variants exhibit different physical properties, which are reflected in crystal morphology, optical characteristics, and among others also in bioavailability. That is why precise solid-state characterization and the correct identification of polymorphs is a vital requirement.

The crystal structure of the well-known simvastatin Form **I** was previously reported [1]. The changes indicating occurrence of two new phases (**II** and **III**) were observed in the course of the preliminary ss-NMR experiments at low temperatures. The phase changes were later confirmed by low-temperature powder diffraction measurements on a laboratory diffractometer. In order to make a precise structure determination of all three existing phases, the synchrotron powder diffraction data and additional solid-state NMR spectra were measured. The individual approaches and challenges of determining this crystal structures are described in this article.

Experimental

Crystallization

Simvastatin (1 g) was dissolved in acetone (4 mL) and *n*-heptane (22 mL) was added. The solution was allowed to stand in an open flask at ambient temperature. The gradual

M. Hušák (✉) · B. Kratochvíl · J. Rohlíček
Department of Solid State Chemistry, Institute of Chemical Technology Prague, 16628 Prague 6, Czech Republic
e-mail: husakm@vscht.cz

A. Jegorov
Teva Czech Industries, Research and Development, Branišovská 31, 37005 Ceske Budejovice, Czech Republic

J. Brus
Institute of Macromolecular Chemistry, Czech Academy of Sciences, Heyrovský sq. 2, 16206 Prague 6, Czech Republic

J. Maixner
Central Laboratories, Institute of Chemical Technology Prague, 16628 Prague 6, Czech Republic

Published online: 09 January 2010

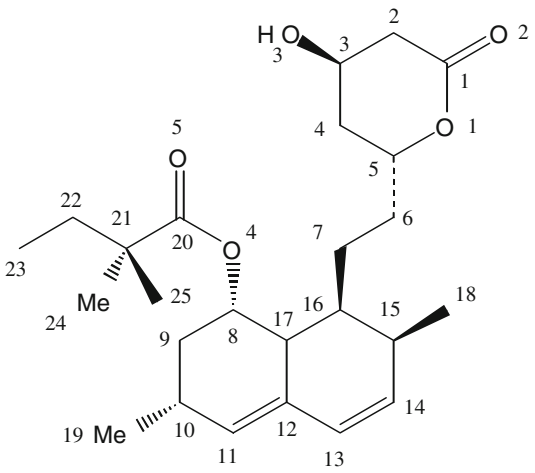

Scheme 1 Structure of simvastatin with the atom numbering as used in [1]

evaporation of acetone facilitated crystallization of simvastatin in the form of white needles.

Thermal methods

Differential scanning calorimetry (DSC) was carried out on a Perkin-Elmer PYRIS 1 system. Aluminum sample pans were used with the amount of the sample about 10 mg. The sample was cooled down (cooling rate 40 °C/min) from the laboratory temperature to −60 °C and tempered 10 min. Then the sample was heated up (heating rate 10 °C/min) up to 30 °C.

Solid-state NMR

All NMR spectra were measured using a Bruker Avance 500 NMR spectrometer (Karlsruhe, Germany, 2003) in 4-mm ZrO_2 rotors. Magic angle spinning (MAS) speed was 11 kHz, nutation frequency $B_1(^1H)$ field for cross polarization was 62.5 kHz, contact time was 2 ms, and repetition delay was 4 s. TPPM (two-pulse phase-modulated) decoupling [2] was applied during the detection period. The phase modulation angle was 15°, and the flip-pulse length was 4.8 μs. The applied nutation frequency of $B_1(^1H)$ field was $\omega 1/2\pi = 89.3$ kHz. High-quality NMR spectra were obtained with accumulation of 128–256 scans. Variable-temperature ^{13}C CP/MAS NMR spectra were measured within the temperature range from 330 to 220 K. The temperature calibration correcting frictional heating of the sample was performed [3]. The ^{13}C scale was calibrated with glycine as the external standard (176.03 ppm—low-field carbonyl signal).

X-ray synchrotron powder data measurement

The powder diffraction data measurement was done on BM01B beamline (Swiss-Norwegian Beamlines) at the ESRF, Grenoble. The beamline uses a channel-cut monochromator Si (111) for wavelength selection. The beam size at the sample is 35 × 3 mm^2. The 2-circle diffractometer used in this experiment was equipped with six counting chains, meaning that six complete patterns were collected simultaneously, with an offset in 2θ. The angular offsets between the detectors are kept very small (∼1.1°) in order to keep the total data collection time to a minimum. A Si-111 analyzer crystal was mounted in front of each detector (NaI scintillation counter), resulting in an intrinsic resolution (FWHM) of approximately 0.01° at a wavelength of 1 Å. Before the measurement the diffractometer was calibrated using LaB_6 standard sample and the value of wavelength was checked (0.6996 Å).

The powder sample was placed in a 1-mm capillary made from Hilgenberg non-diffracting low absorption glass (catalogue No. 50). For the low-temperature measurement the capillary with the sample was cooled by gas nitrogen from a CryoStream cooler.

Before the final measurement targeted on structure data determination, we had made a series of 12 fast measurements in 6.5205–13.100500° 2θ with 0.0035° step at different temperatures in 287–150 K ranges. The results of this measurements confirmed that the phase changes are fully reversible. Indication of **I** → **II** phase change was found at the scan made at 261 K. Indication of **II** → **III** phase change was at first found at the scan made at 223 K. No indication of any additional transformation of phase **III** to another one was found until the lowest temperature scan (150 K) (Fig. 1).

The high-resolution scan targeted for structure determination were done at room temperature (for know known phase **I**), at 258 K (phase **II**) and at 150 K (phase **III**). The recording at 150 K was complicated by ice formation on the capillary witch was impossible to avoid experimentally. The capillary was rotating during the measurement. The diffractogram was measured from 0.515° to 27.5° 2θ with 0.0025° step scan and the sample was irradiated 1 s per step. The data from all six detectors were finally binned (based on calibrated scale factor for each detector).

Structure solution and refinement from powder data

From the first look on the data, it was clear that the phases **II** and **III** show very similar powder pattern as the phase I. The phase's similarity was indicated by the full phase change reversibility as well. So the structure solution process was extremely simplified. For the phase **II** it was possible to use the structure of phase **I** as a starting model. The indexation of phase **III** indicated change from orthorhombic to monoclinic system and change from $P2_12_12_1$ space group to $P2_1$ group. Even in this case it was possible to derive enough good starting model form the phase **I** by

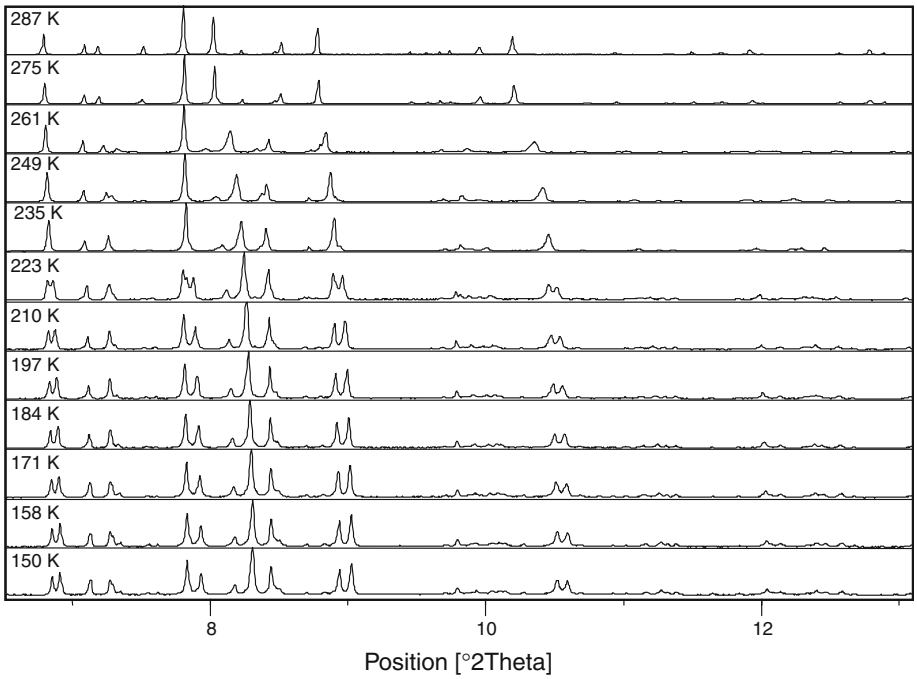

Fig. 1 Results of the fast powder diffraction measurements in the 287–150 K ranges

making two molecules in asymmetric unit cell to refine independently. The phase **I** shows a disorder in the side chains. Modeling of the powder record of phase **I** shows the model with disorder fits to the experimental powder data significantly better than the model without disorder. Unfortunately, because of low data/parameters ratio we were not able to model the phases **II** and **III** as disordered structures so for the starting models for phases **II** and **III** we had used the conformation of **I** with the higher occupancy factors.

The structure refinement was done in Accelrys Material Studio software namely the Reflex Plus module [4]. As the first phase of the refinement we had performed a Le-Bail refinement to obtain good starting profile parameters for the next steps. It should be noticed that a significant line broadening depending on *b*-axis was identified for phase **II** in this step and it was necessary to include this effect in the profile model.

For phase **I** we had only calculated the temperature factor and we did not refined structure obtained from single crystal. The target of this calculation was primary to obtain *R*-factors comparable with other experiments.

The number of structure parameters with should be refined for phases **II** and **III** is higher than the number of observed reflections in the structure, so to be able to refine each atom coordinates, it was necessary to include additional restrains to the refinement. We had used the Material Studio ability to refine simultaneously against powder Rwp factor and against the lattice energy calculated from COMPASS molecular mechanic force field. As the first step we had calculated a Pareto optimization graph showing dependence between Rwp factor and the weight of the energy-based restrains. Based on this graph analysis we had chosen 75% weight of Rwp and 25% weight to the energy-based RE. The decision is arbitrary, because from principal reason it is impossible to determine what is the optimal weighting value. The refinement setup and results are summarized in Table 1.

For phase **III** the experimental record was influenced by ice formation on the capillary during measurement, witch was impossible to avoid experimentally. From this reason regions with possible ice diffraction contribution were rejected from the refinement.

The final agreement between measured and calculated powder records for phases II and III are visualized on Figs. 2 and 3.

Results and discussion

Variable-temperature experiments (DSC and ^{13}C CP/MAS NMR)

DSC is one of the most powerful thermal techniques used to characterize pharmaceutical solids. In general, DSC measurements provide information about solid–solid and solid–liquid transitions and their thermodynamics. Consequently DSC is often utilized to monitor crystal phase stability under various temperature regimes. Analyzing simvastatin the performed DSC measurements showed two events occurring at 232 and 272 K. Both these transitions are instant, sharp, and reversible (endothermic when

Table 1 Crystal data from single crystal measurement of phase **I** taken from [1] and powder diffraction measurement of phases **I–III**

	Single crystal phase **I** [1]	Powder phase **I**	Powder phase **II**	Powder phase **III**
Formula	$C_{25}H_{38}O_5$			
MW	418.57			
Absorption coefficient (mm^{-1})	0.08	0.08	0.08	0.08
Crystal system	Orthorhombic	Orthorhombic	Orthorhombic	Monoclinic
Space group, Z	$P2_12_12_1$, 4	$P2_12_12_1$, 4	$P2_12_12_1$, 4	$P2_1$, 4
a, Å	6.1283(3)	6.1251(1)	6.0914(4)	6.0237(3)
b, Å	17.2964(7)	17.3137(3)	16.727(1)	16.2164(7)
c, Å	22.4659(6)	22.4636(4)	23.147(1)	23.465(1)
β (°)				89.067(2)
T (K)	293	293	258	150
Independent reflections collected	2692	–	–	–
Wavelength (Å)	0.7107	0.6996	0.6996	0.6996
θ range for data collection (°)	0–26	0.515–27.5	0.515–27.5	0.515–27.5
θ range used for refinement (°)	0–26	2.5–20	2.5–20	2.5–20
Reliability factors	$R = 0.072$	Rp = 0.096	Rwp = 0.147	Rwp = 0.154
	Rw = 0.084	Rwp = 0.138	Rp = 0.106	Rp = 0.113
	$S = 1.12$		Rcomb = 0.122	Rcomb = 0.0926
Function minimized	$\sum w(F_o - F_c)^2$	Rwp	75% Rwp, 25% RE	75% Rwp, 25% RE
Weighting scheme	Prince modified Chebychev polynomial	–	–	–
Parameters refined	267	10 profile parameters, 1 structure parameter (structure fixed to single crystal data, only global U(iso) refined)	11 profile parameters, 205 structure parameters (68 positions, global U(iso)	10 profile parameters, 407 structure parameters (136 positions, global U(iso)
Profile function	–	Pseudo-Voigt	Pseudo-Voigt	Pseudo-Voigt
Profile parameters refined	–	U, V, W, NA, NB, zero point, Howard asymmetry, lattice parameters	U, V, W, NA, NB, zero point, Howard asymmetry, lattice parameters, b-axis profile broadening	U, V, W, NA, NB, zero point, Howard asymmetry, lattice parameters
Background model	–	20 parameters polynomial	20 parameters polynomial	20 parameters polynomial
Software used for structure solution and refinement	CRYSTALS [7]	Accelrys Material Studio Reflex [4]	Accelrys Material Studio Reflex [4]	Accelrys Material Studio Reflex [4]

cooled; exothermic when heated) without hysteresis. Therefore, the detected events were attributed to two solid–solid (crystal phase) transitions. Consequently, simvastatin can be found in three crystal modifications: the Form **I** is stable at temperatures higher than 272 K, the Form **II** within the temperature range 272–232 K, and the Form **III** at temperatures below 232 K.

While DSC experiments well-described thermodynamics of the crystal phase transitions, high-resolution solid-state NMR spectroscopy provided site-specific information about these events at atomic resolution. Having unambiguously assigned all ^{13}C NMR signals [5], the variable-temperature ^{13}C CP/MAS NMR spectra easily recognized the molecular sites that are affected by the crystal-phase transformation.

During the cooling of simvastatin a new set of NMR signals appeared at about 272 K (Fig. 4) indicating formation of a new crystal modification (Form **II**). In the temperature range 272–232 K the detected ^{13}C NMR signals exhibit very strong temperature dependences and predominantly signals of methyl groups of the ester tail (carbons No. 23–25) undergo significant broadening and position shifts. In addition, below 242 K these broad signals split into broad doublets which instantly narrow at 232 K (Fig. 4). As just this temperature corresponds with the second crystal phase transition the observed signal

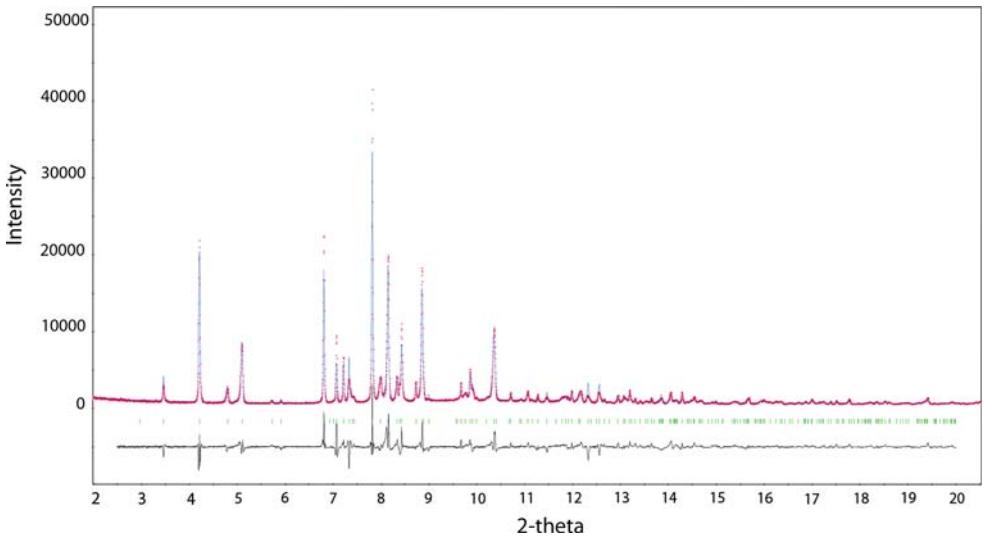

Fig. 2 Agreement between calculated and measured powder diffractogram for phase **II**

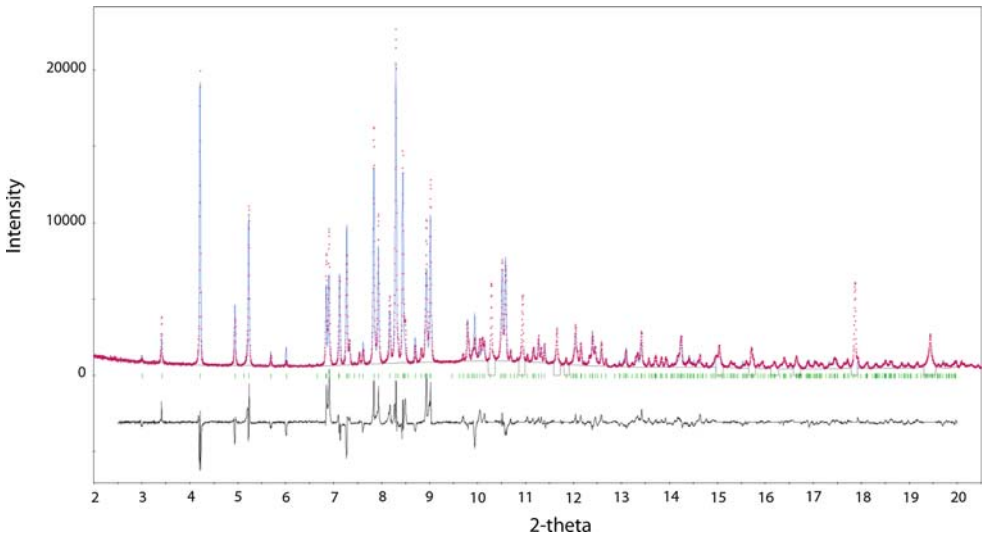

Fig. 3 Agreement between calculated and measured powder diffractogram for phase **III**. Comparison not done in areas with ice diffraction contribution

narrowing reflects formation of the crystal Form **III**. Below the second transition temperature (273 K) the recorded ^{13}C NMR signals did not exhibit significant temperature dependences and the existence of two sets of NMR signals indicates presence of two symmetry independent molecules in the crystal unit (molecules 1 and 2, Form **III**).

From our previous investigations of simvastatin [1, 5] followed that the ester tail undergoes extensive dynamic disorder. Fast jumps or rotational diffusion motions around the axis defined by carbon atoms C20–C21 and C21–C22 occur at room temperature. Consequently, in the time window of NMR experiment (from microseconds to milliseconds) the molecules of simvastatin (Form **I**) do not occupy stable conformations. Only the time-average conformation of the ester tail can be defined by the most probable torsion angles C20–C21–C22–C23 and O4–C20–C21–C22 (Table 2).

As indicated by the broadening and shift of the detected ^{13}C NMR signals of methyl carbons C23, C24, and C25 the time-average conformation of the ester tail is significantly changing below the first transition temperature 272 K. It is well known that isotropic chemical shift allows different aliphatic segment conformations to be identified through the *gamma-gauche* effect. Following the literature [6], the observed changes in isotropic chemical shifts indicate that the time-average conformation of the ester tail in the crystal Form **II** significantly differ form the average conformation of the crystal Form **I** and is strongly a temperature-dependent. With decreasing temperature segmental dynamics of the ester tail is slowed down and chemical exchange between several conformations is clearly reflected by the broadening of NMR signals. The chemical exchange is further slowed down by the sample cooling and as indicated by the appearance of broad doublets two distinct states dominate at temperatures lower than 247 K. The fast chemical exchange is quenched below 242 K. This is indicated by the instant narrowing of the broad doublets when the crystal Form **III** is established. Following from

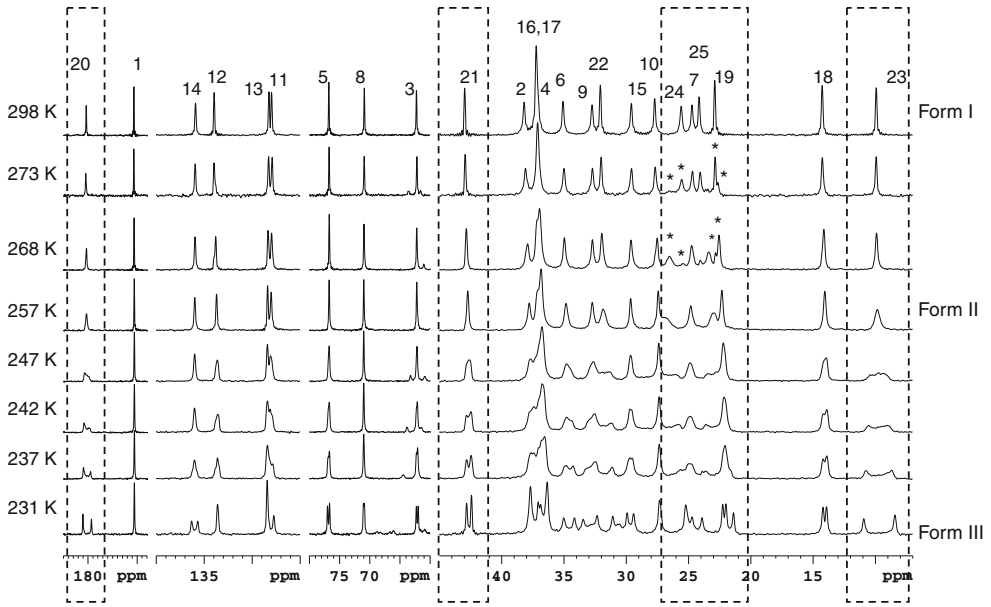

Fig. 4 VT ^{13}C CP/MAS NMR spectra of simvastatin measured within the temperature range from 230 to 300 K. The most affected NMR signals are highlighted by the *dashed boxes*. The temporary splitting of some signals is marked by *asterisks*

Table 2 Comparison of side-chain torsion angles in different simvastatin symmetry-independent molecules

Torsion angle	Form **I** (higher occupancy conformation)	Form **I** (lower occupancy conformation)	Form **II**	Form **III** molecule 1	Form **III** molecule 2
C17–C8–O4–C20	−158.7	−158.7	−159.0	−163.8	−163.0
C8–O4–C20–C21	172.0	172.0	172.6	165.9	173.0
O4–C20–C21–C22	−26.3	155.2	137.5	13.58	48.3
C20–C21–C22–C23	174.8	138.4	172.9	−141.2	−77.6
C17–C16–C7–C6	−169.8	−169.8	−161.8	−159.7	−153.4
C16–C7–C6–C5	174.8	174.8	−163.1	−168.4	−161.2
C7–C6–C5–O1	72.5	72.5	73.4	71.7	68.2

these findings, the crystal Form **II** can be considered as a transient crystal modification of simvastatin that lies between the Form **I** in which the rotation or jumps of the ester tail is not restricted, and the Form **III** in which the dynamic processes are frozen. Only residual dynamic processes indicated by the asymmetric shape of some signals (e.g., carbonyl signal C20) persist below 232 K.

Finally at very low temperature, molecules of simvastatin occupy two distinct conformations in symmetry independent part of the crystal unit (molecules 1 and 2, Form **III**). As follows from integral intensities of the signals in doublets (ca. 1:1) there is no energy preference of a particular conformation. The observed large differences in ^{13}C NMR chemical shifts of methyls C23, C24, and C25 in symmetry independent molecules reach the values of ca. 2.6, 6.0, and ppm 2.6, respectively. These differences can be explained just by the above-mentioned *gamma-gauche* effect. While in the molecule 1, methyl group C23 rather occupies approximately *gauche*$^+$ and *gauche*$^-$ conformations with respect to methyl groups C24 and C25; in the molecule 2, the methyl group C23 is twisted to roughly reach *gauche*$^-$ and *trans* conformations with respect to methyl groups C22 and C23, respectively.

In conclusion, segmental dynamics of the ester tail of simvastatin plays key role in understanding of the observed crystal phase transitions; however, detail analysis of the dynamics of simvastatin in all crystal modifications goes beyond the objective of this study and therefore will be subjected to further examination in our subsequent study. Nevertheless the obtained information provided valuable clues for the analysis of XRPD data and subsequent structure refinements.

Structure solution

During the structure refinement of phases **II** and **III**, it was impossible to get really good agreement between the predicted and the measured powder diffraction record. The main reason are disordered part of the side chain ethyl group, which was observed in single crystal structure. It is impossible to describe this effect sufficiently from powder data only. The low parameters/data ratio had forced us to use energy calculations as additional source of data for refinement, unfortunately the energy calculation do not permit to use disordered models. So the obtained structure corresponds to the higher occupancy disorder only.

However, the final *R* factors as listed in Table 1 for phases **II** and **III** are comparable to the value of phase **I** with the disordered introduced so the model can be considered as acceptable.

Comparison of modifications **I**, **II**, and **III**

The comparison of phases **I**, **II**, and **III** can be done based on the lattice parameter and on the conformation of the molecules in the structure. The lattice parameters almost do not change and even transformation to the lower symmetry (monoclinic space group $P2_1$) for **III** does not result in significantly different lattice.

The comparison of the molecules conformation in the structures was done based on analysis of flexible torsion angles (Table 2). It is visible that significant differences are only in the O4–C20–C21–C22 and C20–C21–C22–C23 torsion angles describing the rotation of the side group. The conformation differences are illustrated in Fig. 5 showing the overlap of the main two rigid cycles and flexibility of side parts of the molecule.

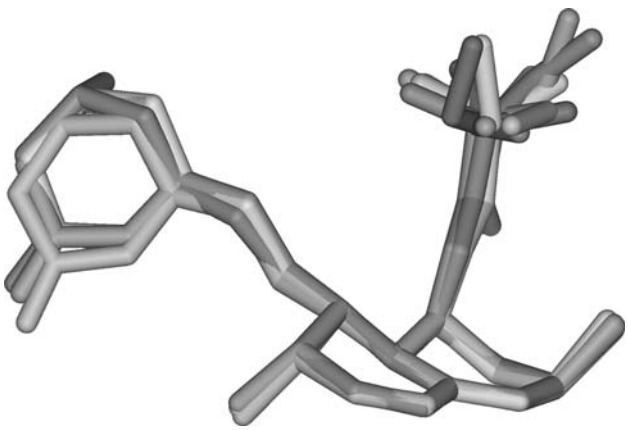

Fig. 5 Comparison of different molecules conformations of simvastatin in phases **I**–**III**

The system of the H-bond is in all phases identical as already described in [1]. The packing is based on only one hydrogen bond O3–H···O5($1 - x$, $y + 1/2$, $1/2 - z$).

Conclusion

Two new low-temperature phases of simvastatin were characterized. There are only slight differences between these phases, but the differences still significantly affect the powder diffraction pattern. It is interesting that this phase changes are fully reversible. From the terminology point of view it would be interesting to discuss, if such slight conformation changes accompanying the phase transformation **I** to **II** are enough to consider the change as a true phase transformation or a change of disorder with the identical phase. However, the energy changes occurring during this process recorded by DSC measurements rather indicated true crystal-phase transition.

In addition, the comparison of solid-state NMR and crystal structure determination from the powder diffraction data indicates that these techniques are complementary and provide different type of information. Whereas X-ray powder diffraction is no doubt powerful technique providing 3-dimensional structure of the molecule, the conformation of flexible or disordered parts is described statically based on the center of electron density only. The limited content of parameters obtained from the powder diffractogram on one hand and the dramatic increase of degrees of conformation freedom associated with the increase of the number of independent molecules on the other hand create the limits of this method. Solid-state NMR crystallography is fairly not so well established technique with respect to the possibility to provide 3-dimensional structure with the resolution comparable with the X-ray diffraction technique; however, ssNMR provides much more clearly the information about the disorders and dynamical processes in the crystal structure.

Supplementary material

The powder diffraction data as well as the results of the structure determination from the powder can be obtained from the first author under request from following e-mail: husakm@vscht.cz.

Crystallographic structure data based on the single crystal diffraction has been deposited in the Cambridge Crystallographic Data Center, CCDC 747933 and CCDC 747932. Copies of this information may be obtained free of charge from The Director, CCDC, 12 Union Road, Cambridge, CB2 1EZ, UK (fax: +44-1223-336033; e-mail: deposit@ccdc.cam.ac.uk or http://www.ccdc.cam.ac.uk).

Acknowledgments This study was supported by the Grant of the Czech Grant Agency (GAČR 203/07/0040), grant from the Grant Agency of the Academy of Sciences of the Czech Republic (IAA400500602), and by the research program MSM6046137302 of the Ministry of Education, Youth and Sports of the Czech Republic. We also thank the Ministry of Education, Youth and Sports for financial support (Grant No. 2B08021). We acknowledge the European Synchrotron Radiation Facility for provision of synchrotron radiation facilities and we would like to thank Denis Testemale for assistance in using beam line BM01B.

References

1. Čejka J, Kratochvíl B, Císařová I, Jegorov A (2003) Acta Cryst C59:o428
2. Bennett AE, Rienstra CM, Auger M, Lakshmi KV, Griffin RG (1995) J Chem Phys 103:6951
3. Brus J (2000) Solid-State Nucl Magn Reson 16:151
4. Reflex Plus, Accelrys Material Studio 4.4, Accelrys Software Inc, 2008
5. Brus J, Jegorov A (2004) J Phys Chem A 108:3955
6. Zemke K, Schmidt-Rohr K, Spiess HW (1994) Acta Polym 45:148
7. Betteridge PW, Carruthers JR, Cooper RI, Prout K, Watkin DJJ (2003) Appl Cryst 36:1487